Macromolecules

Article

pubs.acs.org/Macromolecules

Synthesis and Photophysical and Electroluminescent Properties of Poly(1,4-phenylene−ethynylene)-*alt*-poly(1,4-phenylene−vinylene)s with Various Dissymmetric Substitution of Alkoxy Side Chains

Nassima Bouguerra,[†,‡] Aleš Růžička,[§] Christoph Ulbricht,[‡] Christina Enengl,[‡] Sandra Enengl,[‡] Veronika Pokorná,[§] Drahomír Výprachtický,[§] Elisa Tordin,[‡] Razika Aitout,[†] Věra Cimrová,*[,§] and Daniel Ayuk Mbi Egbe*[,‡]

[†]Department of Chemical Engineering, Electrochemistry, Corrosion and Energetic Valorization Laboratory, A. MIRA University, Targa Ouzemmour, 06000 Bejaia, Algeria

[‡]Linz Institute for Organic Solar Cells, Physical Chemistry, Johannes Kepler University Linz, Altenbergerstrasse 69, 4040 Linz, Austria

[§]Institute of Macromolecular Chemistry, Academy of Sciences of the Czech Republic, Heyrovský Sq. 2, 162 06 Prague 6, Czech Republic

Supporting Information

ABSTRACT: The synthesis and characterization of a set of conjugated polymers, poly(1,4-phenylene−ethynylene)-*alt*-poly(1,4-phenylene−vinylene)s (PPE−PPVs), with a dissymmetrical configuration (partial or total) of alkoxy side chains is reported. Five new polymers bearing octyloxy and/or octadecyloxy side chains at the phenylene−ethynylene and phenylene−vinylene segments, respectively, were obtained. Two symmetrical substituted polymers were used for comparison. Polymers with weight-average molecular weight, M_w, up to 430 000 g/mol and degree of polymerization between 17 and 322 were obtained by a Horner−Wadsworth−Emmons olefination polycondensation reaction of the respective luminophoric dialdehydes and bisphosphonates. As expected, identical conjugated backbones in all polymers results in very similar photophysical response in dilute solution, with high fluorescence quantum yields between 50% and 80%. In contrast, the thin film properties are dependent on the combinatorial effects of side chain configuration, molecular weight, and film thickness parameters, which are the basis of the resulting comparison and discussion.

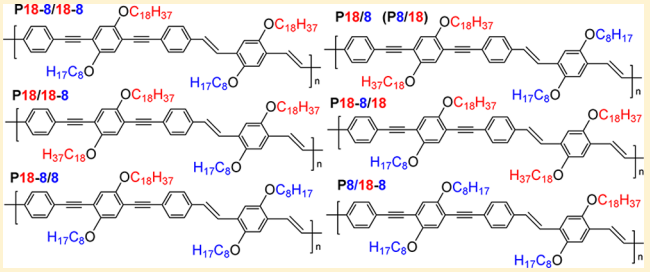

INTRODUCTION

In recent years, intense research efforts have been dedicated to the synthesis and the study of soluble semiconducting π-conjugated polymers.[1−5] Because of their tunable photophysical and electronic properties[6−10] in combination with good processability, flexibility[3,6,11] and stability,[12,13] they hold high promise for advanced electronics and photonics.[7,14] A broad variety of applications have been proposed, including nonlinear optics,[14−16] optical information storage, organic light-emitting-diodes (OLEDs),[16−21] and electrochromic devices.[22,23] Particular attention is also given to organic field-effect transistors (OFETs)[24,25] and organic photovoltaics (OPVs).[25−27]

Poly(1,4-phenylene−ethynylene)-*alt*-poly(1,4-phenylene−vinylene)s (PPE−PPVs) are an interesting class of materials.[28,29] They combine the intrinsic properties of poly(*p*-phenylene−ethynylene) (PPE) and poly(*p*-phenylene−vinylene) (PPV) in a single polymeric backbone with additional structure-specific features.[30−33] The number, position, and nature (linear, branched, chain length, etc.) of the grafted alkyl and/or alkoxy side chains can significantly influence the properties of the polymers.[33] Thus, the side chains not only facilitate the solubility,[33] but can also remarkably affect optical, electronic and charge carrier transport, in particular in the solid state.[34,35]

Over the years an extensive number of PPE−PPVs functionalized symmetrically with alkoxy side chains at the phenylene−ethynylene (PE) and the phenylene−vinylene (PV) segments have been described. These polymers can be labeled with P*n*/*n*′, where *n* and *n*′ represent the number of carbons in the alkoxy side chains attached to the PE ($R_1 = R_2$) and PV ($R_3 = R_4$) segments, respectively. Distinctive effects on the photophysical properties have been observed, in particular in solid state, namely the color appearance of the polymers, the absorption and emission characteristics, as well as the quantum yields of optical transitions.[7,36,37] For instance, while the vast majority of the P*n*/*n*′ polymers (e.g., P18/*n*′, *n*′ = 4−7, 9, 10, 12, 14, 16, 18; P17/7, P19/9; P*n*/8, *n* = 12−15) exhibit a yellow color in the solid state, specific side chain combinations

Received: October 14, 2015
Revised: January 4, 2016
Published: January 14, 2016

DOI: 10.1021/acs.macromol.5b02267
Macromolecules 2016, 49, 455−464

Scheme 1. Synthesis of Bisphosphonate (3ab) and Luminophoric Dialdehydes (7ab and 8ab)

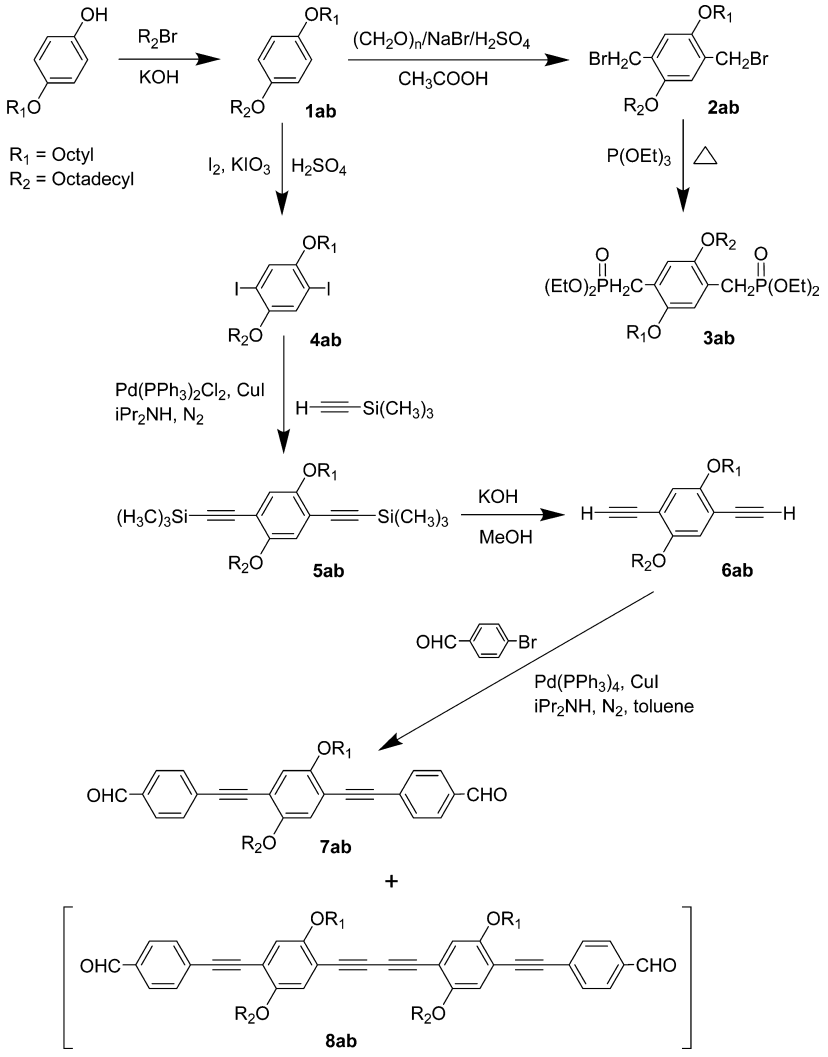

Scheme 2. Synthesis of PPE–PPVs (P) using the Horner–Wadsworth–Emmons Polycondensation Reaction of Bisphosphonates (3) and Dialdehydes (7)

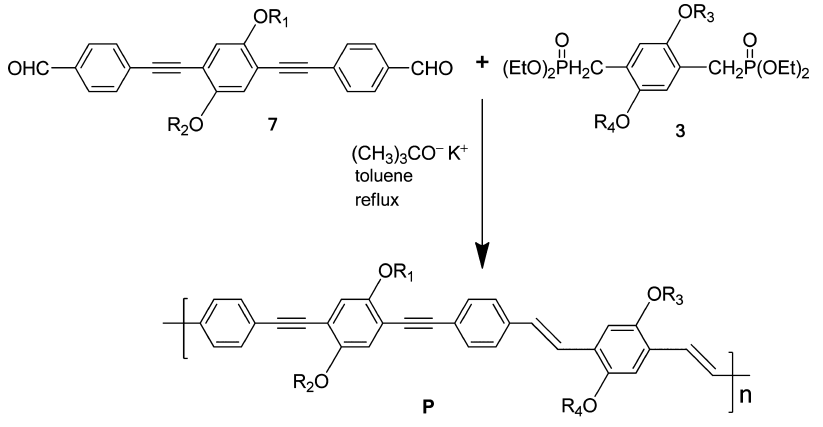

P18/8: $R_1 = R_2 = C_{18}H_{37}$, $R_3 = R_4 = C_8H_{17}$
P8/18: $R_1 = R_2 = C_8H_{17}$, $R_3 = R_4 = C_{18}H_{37}$
P18-8/18-8: $R_1 = R_3 = C_{18}H_{37}$, $R_2 = R_4 = C_8H_{17}$
P18/18-8: $R_1 = R_2 = R_3 = C_{18}H_{37}$, $R_4 = C_8H_{17}$
P8/18-8: $R_1 = R_2 = R_3 = C_8H_{17}$, $R_4 = C_{18}H_{37}$
P18-8/18: $R_1 = R_3 = R_4 = C_{18}H_{37}$, $R_2 = C_8H_{17}$
P18-8/8: $R_1 = R_3 = R_4 = C_8H_{17}$, $R_2 = C_{18}H_{37}$

DOI: 10.1021/acs.macromol.5b02267
Macromolecules 2016, 49, 455–464

(P16/6, P16/8, P17/8, P18/8, and P19/8) cause the precipitated polymers to take on an orange appearance.[1,31,37]

To further explore the impact of variations in the side chain configuration, we report on PPE–PPVs with dissymmetric substituted PE ($R_1 \neq R_2$) and/or PV building blocks ($R_3 \neq R_4$). In this paper, we describe the synthesis and detailed characterization of five new conjugated polymers with different combinations of octadecyloxy ($OC_{18}H_{37}$) and octyloxy (OC_8H_{17}) substituents, including syntheses of two new polycondensation monomers **3ab** and **7ab** (Scheme 1 and 2). The electrochemical, photophysical and electroluminescent properties of these new materials are investigated and compared to newly synthesized batches of known reference polymers with symmetrical substitution—**P18/8** ($R_1 = R_2$ = octadecyl; $R_3 = R_4$ = octyl) and **P8/18** ($R_1 = R_2$ = octyl; $R_3 = R_4$ = octadecyl; Scheme 2).

RESULTS AND DISCUSSION

Synthesis and Characterization. The synthesis of the polymers **P** via the Horner–Wadsworth–Emmons (HWE) olefination reactions requires the preparation of the respective bisphosphonates **3** and luminophoric dialdehydes **7**. The polycondensation monomers **3** and **7** were synthesized in multistep reaction sequences starting either from hydroquinone, for symmetric substituted compounds **3aa**, **3bb**, **7aa**, and **7bb** (aa, $R_1 = R_2$ = octyl; bb, $R_1 = R_2$ = octadecyl) as described elsewhere,[16] or from 4-octyloxyphenol, for the new dissymmetric substituted compounds as depicted in Scheme 1.

The synthesis of the bisphosphonate **3ab** involved a sequence of Williamson etherification, bromomethylation and Michealis–Arbuzov reaction. Dialdehyde **7ab** was also synthesized in several steps in analogy to the literature for the symmetric substituted compounds.[38] The diiodination of 1-octadecyloxy-4-octyloxybenzene **1ab** was followed by a Pd-catalyzed Sonogashira cross-coupling reaction with trimethylsilylacetylene, the deprotection of the acetylene units, and finally another Sonogashira reaction leading to the desired product **7ab**, which was obtained as bright yellow substance alongside a small amount of diyne dialdehyde **8ab**. For the purification of the materials, column chromatography and/or recrystallization were performed. The desired polymers **P** were obtained by reacting 2,5-dialkoxy-*p*-xylylene-bis(diethylphosphonates) (**3**) and 1,4-bis(4-formylphenylethynyl)-2,5-dialkoxybenzenes (**7**) in various combinations (Scheme 2).

Olefination reactions via HWE are commonly characterized by high reaction rate, high yields, high selectivity (high preference of trans (*E*) double bonds), and very low structural defects.[6] In contrast to cross-coupling reactions such as Heck, Sonogashira, Suzuki and Stille, a metal catalyst, which might be problematic during purification, is not required. All polycondensation reactions except one were performed within a 1 h reaction time. The synthesis of the polymer with the fully dissymmetric side chain distribution (**P18–8/18–8**) was repeated with an extended reaction time (by 25 min) in order to obtain a high molecular mass batch of this material (**P18–8/18–8a**).

The structure and purity of the synthesized materials were verified by NMR spectroscopy (^{1}H and ^{13}C NMR). The spectra of the synthesized intermediates and polycondensation monomers are characterized by well resolved and defined signals. Despite the combination of substituents with different alkyl chain lengths in the new compounds, the recorded peak patterns show a high resemblance to the spectra of the uniformly substituted materials. Figure 1 displays the ^{1}H NMR spectrum of the new dialdehyde **7ab** and of the polymer it was used to synthesize, **P18–8/18–8**.

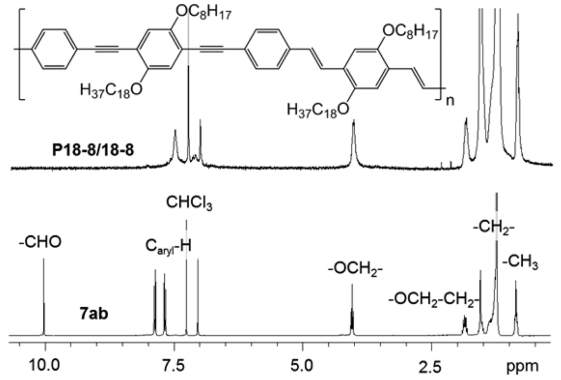

Figure 1. ^{1}H NMR spectra stack of the dialdehyde **7ab** (bottom) and of the corresponding polymer **P18–8/18–8** (top) recorded in $CDCl_3$ at 300 MHz.

The methyl and the methylene proton signals of the alkyl chains appear in the high-field region between 0.86 and 1.89 ppm. The signals of the methylene protons at the carbon adjacent to oxygen are found at approximately 4 ppm. Further downfield, between 7 and 7.8 ppm, the aromatic proton signals arise. In the spectrum of the polymer, characteristic signals of the polycondensation monomers (dialdehyde, ~10 ppm (–CHO); bisphosphonate, ~3.3 ppm ($-H_2CP$)) are absent. In addition, the loss of signal resolution and the strong broadening of the signals are clear indications of the formation of polymer material. The spectrum suggests an all *trans* (*E*) configuration of the polymer. Peaks indicating the presence of vinylenic double bonds with a *cis* (*Z*) configuration are not observed.[38b] For the comprehensive investigation of the five new polymers, infrared (IR) and Raman spectroscopic measurements were performed. Figure 2(top) depicts the IR spectra of all polymers bearing dissymmetric side chains. The spectra show a very weak band in the range of 3070 to 3000 cm^{-1} that is assigned to arylene and vinylene vibrations (vw,

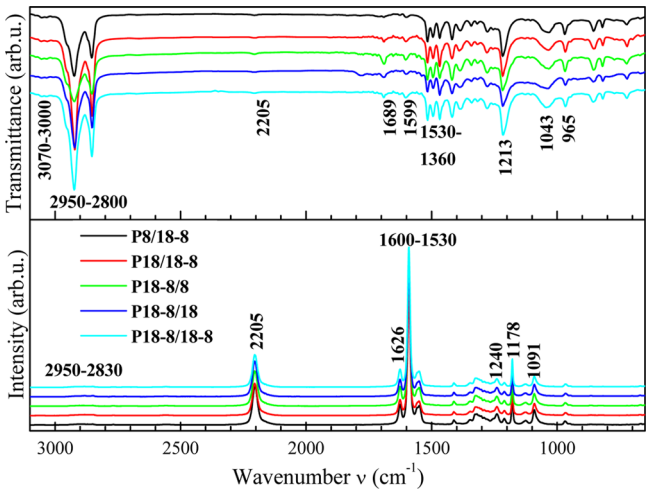

Figure 2. ATR-FTIR spectra plotted in transmittance (top), and Raman spectra (bottom) of the new polymers with dissymmetric side chains.

DOI: 10.1021/acs.macromol.5b02267
Macromolecules 2016, 49, 455–464

−C_{aryl}−H and vinylene −C═C−H), and very strong −C−H vibration peaks between 2950 and 2800 cm^{-1} (vs, −C−H). The weak ethynyl band appears at approximately 2205 cm^{-1} (w, −C≡C−). Two weak peaks located at 1689 and 1599 cm^{-1} originate from vinylenic vibration (w, vinylene−C═C−), and the peaks in the range between 1530 and 1360 cm^{-1} are attributed to aromatic elements (w, aromatic−C═C−). Signals at 1213 cm^{-1} (strong) and 1043 cm^{-1} (medium) are attributed to the alkoxy functionalities (s, m C_{aryl}−OR). The band at 965 cm^{-1} is assigned to the vinylene double bonds with *trans* (*E*) configuration. Signals indicating the presence of *cis* (*Z*) configuration were not identified.[38b]

In the Raman spectra (Figure 2, bottom) a very weak signal in the range of 2950 to 2830 cm^{-1} is observed and assigned to C−H vibrations of the aliphatic chains (vw, −C−H). The strong peak at 2205 cm^{-1} originates from ethynyl units (s, −C≡C−), while the signals at 1626 cm^{-1} and in the range from 1600 to 1530 cm^{-1} are assigned to vinylenic (m, vinylene−C═C−) and aromatic features (vs, aromatic−C═C−), respectively. The alkoxy functionalities appear in the peaks at 1240 and 1091 cm^{-1} (w, C_{aryl}−OR). A strong peak at 1178 cm^{-1} is attributed to the alkyl chains (s, −C−C−).

The weight-average molecular weight (M_w), polydispersity index (PDI) and degree of polymerization (P_n) of the new polymers were determined by size exclusion chromatography (SEC) measurements. The SEC results are summarized in Table 1, and the SEC curves of the polymers under study are

Table 1. Characterization Data for the Polymers under Study (M_w is the Weight-Average Molecular Weight, PDI the Polydispersity Index, and P_n the Polymerization Degree)

polymer	M_w [a] (g/mol)	PDI	P_n	yield (%)
P18/8	20100	2.1	17	71
P8/18	48900	4.3	41	50
P18/18−8	37800	2.1	28	66
P8/18−8	33300	2.7	31	71
P18−8/18	88800	2.6	66	83
P18−8/8	89700	4.9	85	70
P18−8/18−8	34600	3.1	26	76
P18−8/18−8a	431000	4.1	322	86

[a]Measured by SEC in tetrahydrofuran (THF) as the mobile phase, polystyrene standards were used for calibration.

shown in Supporting Information (Figure S3). The synthesized polymers exhibit M_w values between 20 100 and 89 700 g/mol with P_n between 17 and 85, and polydispersity indexes between 2.1 and 4.9, except **P18−8/18−8a** which has the highest weight M_w = 431 000 g/mol with PDI of 4.1 and a corresponding P_n of 322.

Photophysical Properties. The photophysical properties of the new polymers bearing dissymmetric alkoxy side chains together with two polymers **P18/8** and **P8/18** bearing symmetric alkoxy side chains were studied in solutions and thin films. Absorption and photoluminescence (PL) emission spectra measured in tetrahydrofuran (THF) solution are displayed in Figure 3, and their characteristic data summarized in Table 2.

Absorption spectra exhibited a broad absorption band with maxima in the range 440−455 nm corresponding to the absorption of the $\pi-\pi^*$ transition of the conjugated backbone. The maximum positions correlate well with the M_w of the polymers (see Tables 1 and 2), except for the blue-shifted

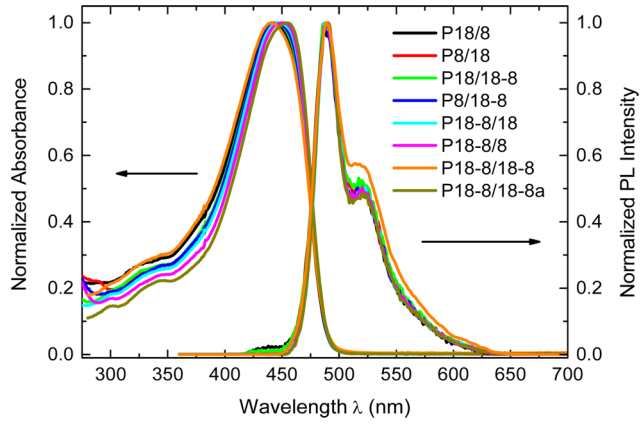

Figure 3. UV−vis absorption and PL emission spectra of the polymers under study measured in dilute THF solution.

Table 2. Photophysical Properties of the Polymers Measured in Dilute THF Solutions (λ_{absmax} Absorption Maximum, λ_{PLmax} Emission Maximum, $\lambda_{PLexcmax}$ Maximum of Excitation Spectra, and η_{PL} Photoluminescence Quantum Yield)

polymer	λ_{absmax} (nm)	λ_{PLmax} [a] (nm)	$\lambda_{PLexcmax}$ [b] (nm)	η_{PL}
P18/8	443	487, 520sh	444	0.70
P8/18	447	489, 521sh	448.5	0.64
P18/18−8	445	488, 517sh	443.5	0.66
P8/18−8	444	487, 521sh	443.5	0.71
P18−8/18	450	489, 520sh	443.5	0.63
P18−8/8	451	490, 520sh	446	0.74
P18−8/18−8	440	488, 516sh	444	0.53
P18−8/18−8a	455	490, 522sh	451	0.64

[a]Excitation wavelength at λ_{absmax} [b]Emission wavelength at λ_{PLmax}

maximum of the **P18−8/18−8** absorption compared with **P18/8** with a lower M_w. One can assume the influence of the dissymmetrical alkyl chains on the backbone conjugation. **P18−8/18−8a** with the highest M_w exhibits an approximately 15 nm red-shift of the absorption maximum compared to **P18−8/18−8** of the same chemical structure but has a lower M_w. When comparing the absorption spectra of the polymers **P18/18−8**, **P8/18−8** and **P18−8/18−8** with similar M_w, a blue shift of **P18−8/18−8** compared to the other ones is observed, which indicates that the dissymmetry of the side chains slightly influences the backbone conjugation as already mentioned above. PL emission spectra in THF solution are of similar shapes, with maxima located at 488−490 nm and a shoulder at approximately 520 nm reflecting the vibronic structure. The PL emission maxima differ only slightly between polymers in a similar manner to the absorption maxima. There are similarities between PL excitation and absorption spectra. PL quantum yields, η_{PL}, of the new polymers are in the range 0.50−0.80. There is no straightforward dependence of the absorption and PL in dilute solution on the combination of side chains.

To discuss the results in detail one should take into account differences in M_w of the polymers under study and discuss the possible influence of the various side chain combinations of polymers with similar M_w. Comparison of the polymers necessitates a division into groups with similar M_w. Comparing **P18−8/18** and **P18−8/8** η_{PL} values, a slight influence of the length of the symmetrical side chains on the vinylene segment is observed. A similar influence is seen on the ethynylene segment when the **P18/18−8** and **P8/18−8** data are

DOI: 10.1021/acs.macromol.5b02267
Macromolecules 2016, 49, 455−464

compared. In both cases the **P18−8/8** and **P8/18−8** polymers with shorter alkyls on vinylene and ethynylene segments, respectively, exhibit a slightly higher η_{PL} values than those of polymers **P18−8/18** and **P18/18−8** with longer alkyls. The absorption and PL results for **P18/8** solution correlate well with the results obtained by previous studies of chloroform solutions of **P18/8** with a higher M_w (M_w = 115 600 g/mol, PDI = 3.77, $P_n \sim 26$)[1] and of **P18/8** with a similar M_w.[35]

Absorption and photoluminescence spectra measured in thin films are displayed in Figure 4 and 5, respectively, and characteristic data summarized in Table 3. The thin film absorption is red-shifted compared with the polymer absorption in solution, which indicates influence of intermolecular interactions in solid state. Contrary to the photophysical properties of the solution, a clear influence of the side chain combination on photophysical behavior is observed in solid state.

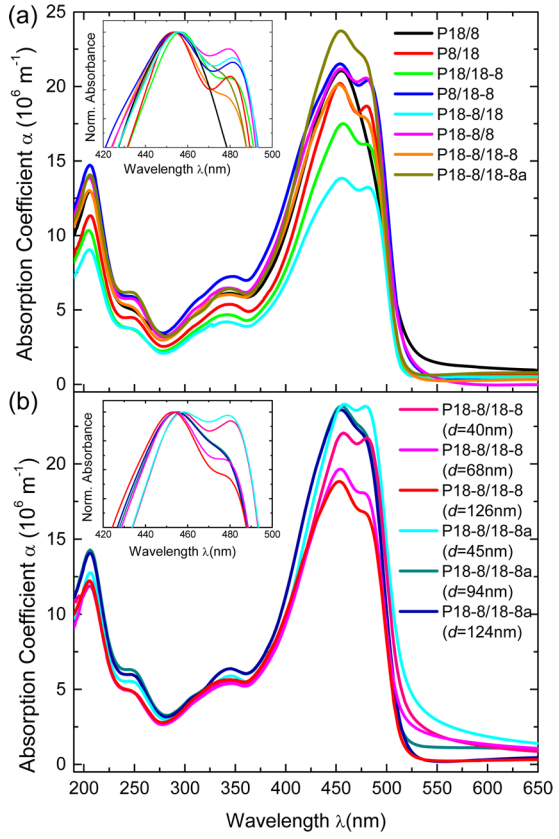

Figure 4. Absorption spectra of thin films of: (a) all polymers under study and (b) **P18−8/18−8** and **P18−8/18−8a** with various thicknesses.

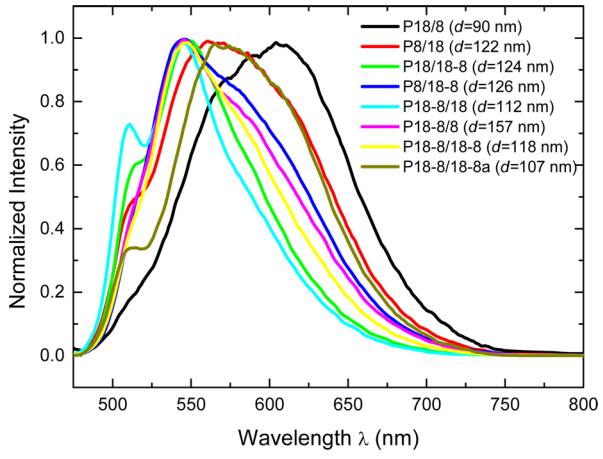

Figure 5. PL spectra of thin films of all polymers under study.

Figure 4a shows the absorption spectra of thin films of all polymers under study, and Figure 4b demonstrates the influence of film thickness on the absorption for selected polymers. The main absorption maxima in thin films are located in the range 453−455 nm for thicker films and slightly red-shifted for thinner films. A second maximum or shoulder at approximately 480−484 nm is well resolved in the absorption spectra of all polymers except **P18/8**. This fact demonstrates the influence of various combinations of side chains on the intermolecular interactions of conjugated segments. The contribution of the absorption of the first and second peak for the same polymer depends on the film thickness. In the measured range of the thicknesses, the absorbance of the second peak increases with decreasing film thickness for all polymers under study except **P18/8**, for which the absorption spectrum lacks a second peak as already mentioned above. Absorption coefficient values are higher for the thinner films. An example is shown in Figure 4b and its inset for **P18−8/18−8** and **P18−8/18−8a**. It should be noted that the value of absorption coefficient evaluated from transmission measurements could be also influenced by reflection losses. This effect is particularly noticeable in the spectral region corresponding to the long wavelength tail.[39] The changes observed in the absorption spectra for different film thicknesses cannot be fully accounted for by reflection losses therefore morphology differences between films are taken into account and discussed. One can assume that the spin-coating process induces an orientation of main chains in-plane more pronounced in thinner films which could explain the higher absorption. An influence of alkyl chain length on the absorption is also detected. The absorption coefficients of thin films made of **P18/18−8** or **P18−8/18** with longer symmetrical alkyl chains are lower than those of thin films made of **P8/18−8** or **P18−8/8** with shorter symmetrical alkyl chains. It correlates well with the higher volume of the alkyl chains in **P18/18−8** or **P18−8/18** than in **P8/18−8** or **P18−8/8**.

The PL emission spectra of thin films shown in Figure 5 differ in the shape and exhibit red-shifts compared with the PL emission in solutions, for which similar PL emission spectrum shapes were observed for all polymers. PL excitation spectra of thin films follow roughly the absorption ones, but possess a better resolution of the vibration structure. The most pronounced PL emission maximum red-shift was observed in the **P18/8** PL spectrum, which exhibits a broad, featureless emission band and a very large Stokes shift (152 nm), characteristics of excimers or aggregates in the solid state.[40] The PL emission maxima of the other polymers are blue-shifted compared to those in the **P18/8** PL spectrum. Relative PL efficiency of thin films, ϕ_{PLrel}, is introduced for a PL efficiency comparison of the polymers under study relatively to each other. New polymers possessing dissymmetric side chains, and also **P8/18** with symmetrical side chains with the longer ones on PV building blocks, exhibit higher ϕ_{PLrel} in thin films than that of **P18/8** thin films. Further, we compare the data from several points of view with respect to various side chain combinations, taking into account polymer M_w variation.

DOI: 10.1021/acs.macromol.5b02267
Macromolecules 2016, 49, 455−464

Table 3. Photophysical Properties of the Polymers Measured in Thin Films (λ_{absmax} Absorption Maximum, λ_{PLmax} Emission Maximum, $\lambda_{PLexcmax}$ Maximum of Excitation Spectra, ϕ_{PLrel} Relative Photoluminescence Efficiency, and d Film Thickness), Where Main Maxima Are Printed Boldface

polymer	d (nm)	λ_{absmax} (nm)	λ_{PLmax} [a] (nm)	$\lambda_{PLexcmax}$ [b] (nm)	ϕ_{PLrel} [a]
P18/8	23	**461**	**605**	**446**, 482	
	90	**455**	**601**	426, **449**, 486	0.17
P8/18	52	**455**, 482	513 sh, **541**	**448**, 483	
	122	**454**, 480	509 sh, **552**	**442**,486	0.37
P18/18−8	28	461, **484**	517 sh, **543**	**458**, 484	
	124	**457**, 480	513 sh, **547**	**444**, 487	0.44
P8/18−8	56	**456**, 483	513 sh, **541**, 578	**449**, 484	
	126	**454**, 481	**544**	445, **484**	1.0
P18−8/18	43	458, **484**	**513**, 543	**451**, 484	
	112	**456**, 481	512, **543**	447, **485**	0.30
P18−8/8	68	**456**, 480	**546**	**448**, 484	
	157	**455**, 480	**544**	**443.5**, 487	0.54
P18−8/18−8	39	**458**, 480	**542**	**449**, 483	
	118	**453**, 479 sh	**546**	**443**, 484	0.51
P18−8/18−8a	107	**455**, 475 sh	514 sh, **570**	458, **486**	
	155	**454**, 478 sh	515 sh, **549**	**444**, 486	0.58

[a]Excitation wavelength at 445 nm. [b]Emission wavelength at λ_{PLmax}.

The comparison of the data obtained for **P18/8**, **P8/18**, and **P18−8/18−8** polymers with the same molar weight of repeat unit with various combinations of side chain positions reveals that exchange of the symmetrical side chain lengths on the PV and PE units increases the value of ϕ_{PLrel} by about a factor of 2 in **P8/18** if the longer side chains are located on PV units, and further by about a factor of 3 for **P18−8/18−8** with dissymmetric side chains on the both units. The shape of both the absorption and emission spectra of the **P18/8**, **P8/18** and **P18−8/18−8** polymers differ as shown in Figure 6a. PL emission maxima of **P8/18** with the longer side chains located on PV units and of **P18−8/18−8** with dissymmetric alkyl chains are blue-shifted compared with that of **P18/8**. The thin film made of **P18−8/18−8a** with higher M_w exhibited a slightly higher ϕ_{PLrel} and red-shifted PL maximum compared **P18−8/18−8** thin film (see Figure 6b). PL emission spectra of **P18/18−8**, **P8/18−8**, **P18−8/18**, **P18−8/8** with longer or shorter symmetric alkyls on ethynylene or vinylene segments are shown in Figure 6c and d. The shapes of the PL spectra are similar for thin films of **P18/18−8** and **P18−8/18** (same molar mass of repeat unit), but differ from those of thin films made of **P8/18−8** and **P18−8/8** with the same molar mass of the repeat unit but lower than that of the **P18/18−8** and **P18−8/18**. More clearly resolved vibration structure was observed in PL spectra of **P18/18−8** or **P18−8/18** with 3 longer (C_{18}) alkyl chains. Comparison of these polymers demonstrates an influence of the alkyl chain length on their photophysical properties in thin films. Similarly, as in solution, the comparison of **P18−8/18** and **P18−8/8** ϕ_{PLrel} values reveals a slight influence of the length of the symmetrical side chains on the vinylene segment, and similarly the **P18/18−8** and **P8/18−8** data comparison reveals the same for the ethynylene segment. In both cases, the **P18−8/8** and **P8/18−8** polymers with shorter (C_8) alkyls on vinylene and ethynylene segments, respectively, exhibit a slightly higher ϕ_{PLrel} than those for polymers **P18−8/18** and **P18/18−8** with longer alkyls. The introduction of dissymmetric side chains leads to the changes in both absorption and PL spectra of the polymers, reflecting differences in backbone interactions between main chain segments.

Electrochemical Properties. Cyclic voltammetry (CV) measurements were performed to obtain information on the electronic structure of the new polymers. An example of a representative CV curve of **P18−8/18−8** thin films coated on a Pt wire is displayed in Figure 7.

Quasi-reversibility in both oxidation and reduction were observed for all new polymers. The ionization potential (HOMO level), E_{IP}, and electron affinity (LUMO level), E_A, were estimated from the onset potentials, E_{onset}, of the oxidation and reduction peaks on the basis of the reference energy level of ferrocene (4.8 eV below the vacuum level) using the equation E_{IP} (E_A) = |− (E_{onset} − E_{ferr}) − 4.8| eV, where E_{ferr} is the value for ferrocene vs the Ag/Ag^+ electrode. The E_{IP} and E_A values were evaluated as averages from CV curves measured at a scan rate of 50 mV s^{-1} and are given in Table 4. Similar values of the ionization potential, in the range 5.23−5.27 eV, and electron affinity, in the range 2.75−2.79 eV, were measured for all polymers. The electrochemical bandgap values, E_g^{elc} = 2.47−2.5 eV, were evaluated. These results are in good agreement with the optical bandgap values of 2.39−2.46 eV determined from thin film absorption spectra.

Electroluminescence. The new polymers were used to create an active layer in samples of light-emitting devices (LEDs). LEDs with a hole-injecting electrode formed by ITO covered with a PEDOT:PSS layer and an electron-injecting electrode of calcium covered with aluminum (Ca/Al) were prepared and studied. The electroluminescent (EL) spectra of the LEDs are shown in Figure 8. The EL maxima are summarized together with the PL maxima in Table 5.

The electroluminescence of **P18/8** and **P8/18** bearing symmetric alkoxy side chains has already been studied with different luminance efficiencies (0.11[41] or 0.22[31] to 1.79[1]). Our LEDs made of **P18/8** exhibited luminance efficiency values, η_{EL}, in the range of 0.22−0.46 as measured on several LED samples even with the similar active layer thickness. The lower value is consistent with the luminance efficiency of 0.22 reported for LEDs made with similar device configuration using the polymer with similar molar weight.[31] The η_{EL} values for LEDs made of **P8/18** approach the published data of luminance efficiency of 0.12.[41]

DOI: 10.1021/acs.macromol.5b02267
Macromolecules 2016, 49, 455−464

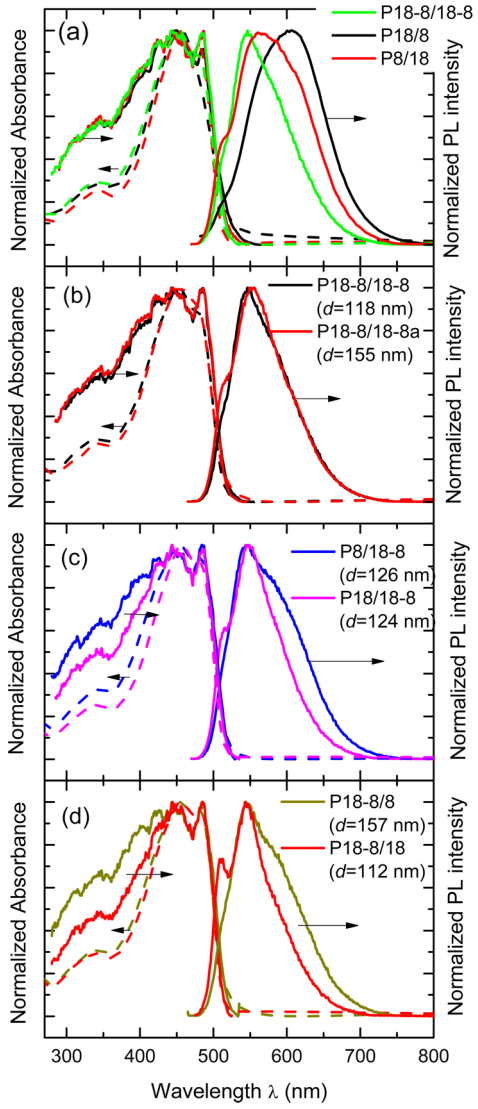

Figure 6. UV−vis absorption (dashed), PL excitation and emission spectra of the polymers under study measured in thin films: (a) **P18/8, P8/18, P18−8/18−8** (polymers with the same molar mass of repeat unit), (b) **P18−8/18−8, P18−8/18−8a** (same polymer with different M_w), and (c, d) **P18/18−8, P8/18−8, P18−8/18, P18−8/8** - comparison of symmetrical alkyl chains increasing or decreasing volume on ethynylene (c) or vinylene (d) segments.

LEDs made using the new polymers **P8/18−8, P18−8/18, P18−8/18−8**, and **P18−8/18−8a** exhibited η_{EL} values comparable to those for LEDs made of **P18/8**, whereas the η_{EL} values of **P8/18**, **P18/18−8**, and **P18−8/8** were less performant. It should be noted that these copolymers have different molar weights, so it is necessary to discuss the results also in relation to the M_w. From this point of view, a comparison of the results obtained for **P18−8/18−8** and **P18−8/18−8a** with two different molar weights shows that the changes in η_{EL} with M_w are not significant. An influence of the length of the symmetrical side chains on the vinylene segment is evident from a comparison of the η_{EL} values of the copolymers **P18−8/18** and **P18−8/8** with very similar molar weights. The devices made using copolymer **P18−8/18** exhibited higher η_{EL} values than those made using **P18−8/8** with the shorter side chains on the vinylene segment. η_{EL} values of **P8/18−8** LEDs are higher than those of **P18/18−8** LEDs,

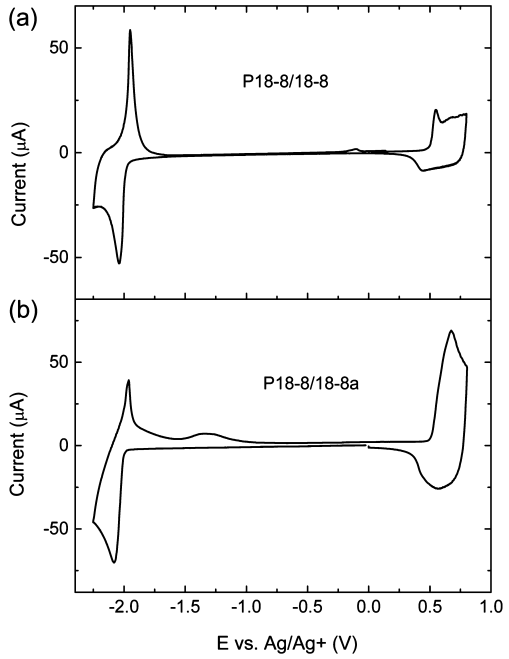

Figure 7. Representative cyclic voltammograms of (a) **P18−8/18−8** and (b) **18−8/18−8a** thin films coated on a Pt wire recorded at a scan rate of 50 mV s^{-1}.

which correlates with the measured ϕ_{PLrel} values of corresponding thin films.

The maximum luminance values of approximately 900 cd m^{-2} were observed from the best devices made with **P18−8/18**. An example of the luminance dependency on the applied voltage is displayed in Figure 9. The higher onset voltages of more than 5 V are caused by an interface barrier, probably higher for electrons, and also can be influenced by a higher active layer thickness. Maxima of the EL spectra are red-shifted compared with those of PL thin film spectra, which indicates that charge trapping takes place in the EL process. On the basis of our various comparison, one can conclude that introducing dissymmetric side chains in both segments influence the EL efficiency, but not in a way that correlates straightforwardly with the PL results. Further optimization of LEDs is needed. The performance can be improved using an active blend layer, such as those reported in our previous papers.[42−45]

CONCLUSION

Five new poly(*p*-phenylene−ethynylene)-*alt*-poly(*p*-phenylene−vinylene)s with a dissymmetrical configuration (partial or total) of octyloxy and/or octadecyloxy chains at the phenylene−ethynylene and/or phenylene−vinylene segments, respectively, and two corresponding polymers with symmetrical configuration were synthesized using polycondensation reactions of the respective dialdehydes and bisphosphonates. The polymers have average molecular weights M_w up to 430 000 g/mol. For all polymers, similar values of the ionization potential (5.23−5.27 eV) and electron affinity (2.75−2.79 eV) were obtained by means of cyclic voltammetry. The values of electrochemical bandgap are similar (2.47−2.5 eV) and in good agreement with the optical bandgap values (2.39−2.46 eV) determined from thin film absorption spectra. Differences in absorption and photoluminescence were found both in solution and in thin films. The influence of various combinations of side chains on absorption and PL emission is more pronounced in

DOI: 10.1021/acs.macromol.5b02267
Macromolecules 2016, 49, 455−464

Table 4. Electronic Properties of the Polymers under Study (E_{IP} Ionization Potential, E_A Electron Affinity, E_g^{elc} Electrochemical Bandgap, and E_g^{opt} Optical Bandgap)

polymer	E_{IP} (eV), − HOMO	E_A (eV), − LUMO	E_g^{elc} (eV)	E_g^{opt} (eV)
P18/8	5.25	2.76	2.49	2.39
P8/18	5.25	2.75	2.50	2.40
P18/18−8	5.23	2.75	2.48	2.44
P8/18−8	5.26	2.79	2.47	2.43
P18−8/18	5.31	2.76	2.55	2.44
P18−8/8	5.27	2.76	2.51	2.44
P18−8/18−8	5.25	2.77	2.48	2.45
P18−8/18−8a	5.23	2.75	2.48	2.46

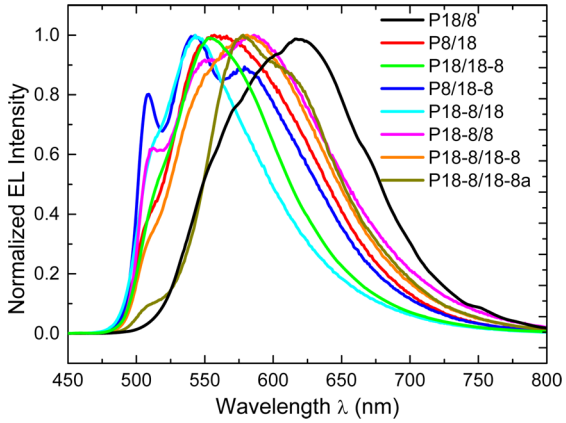

Figure 8. Normalized electroluminescent spectra of LEDs made of polymers under study (LED configuration: ITO/PEDOT:PSS/polymer/Ca/Al).

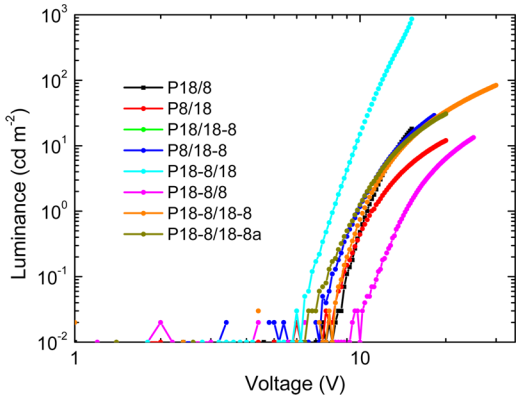

Figure 9. Luminance dependence on the applied voltage measured on ITO/PEDOT:PSS/polymer/Ca/Al LED.

thin films compared to solutions. The PL thin film emission spectra of all new polymers are blue-shifted compared to that of **P18/8** with symmetrical side chains. In thin films, new polymers possessing dissymmetric side chains and **P8/18** with symmetrical side chains with the longer ones on phenylene segment exhibit higher PL efficiency values by a factor of 2−5. Polymer LEDs were prepared and characterized using the new polymers. The introduction of dissymmetric side chains in both segments influences the EL efficiency as shown by various comparisons, but a comparison with the PL results is not straightforward. Charge trapping takes place in the EL process as indicated by the red-shift of EL compared to thin film PL.

EXPERIMENTAL SECTION

1. Materials and Methods. The starting materials were purchased from commercial suppliers such as Sigma-Aldrich and were used without further purification unless specified. Solvents and reaction mixtures were deaerated by bubbling with nitrogen for 1 h prior to use. The polymers with symmetric side chain configuration (**P8/18**, **P18/8**) were synthesized as described in the literature.[6]

^{1}H NMR and ^{13}C NMR spectra were measured in $CDCl_3$ with a Gemini 300 MHz spectrometer at 298 K using trimethylsilane as an internal standard. IR experiments were performed on a Bruker Fourier transform infrared (FTIR) spectrophotometer IFS 66/S with a liquid nitrogen cooled mercury cadmium telluride (MCT) detector in the attenuated total reflection (ATR) mode. All polymers were dissolved in chlorobenzene (VWR chemicals) and then spin-coated onto the ZnSe crystal, which is used as a reflection element for the ATR-FTIR measurements. The crystal was precleaned with diamond paste and then rinsed with acetone in a reflux system before further treatments. For the Raman measurements, all the

Table 5. Electroluminescent Properties of the New Polymers Obtained from LEDs (ITO/PEDOT:PSS/polymer/Ca/Al) characterization (λ_{ELmax} EL Maximum, λ_{PLmax} PL Emission Maximum of Thin Films, Where Main Maxima Are Printed Bold, η_{EL} EL Efficiency and η_{ELmax} Its Maximum Efficiency, and d Polymer Active Layer Thickness)

polymer	d (nm)	λ_{ELmax} (nm)	η_{EL}@15 V (Cd/A)	η_{ELmax} (Cd/A)	λ_{PLmax} (nm)[a]
P18/8	96	**616**	0.22−0.46	0.46	**606**
P8/18	117	**557**	0.07−0.11	0.12	**545**
P18/18−8	115	**556**	0.10	0.11	**545**
P8/18−8	117	509, **543**, 579	0.29−0.32	0.36	**544**
P18−8/18	98	**543**	0.18−0.24	0.24	512, **543**
P18−8/8	142	512, 550, **586**	0.08	0.12	**544**
P18−8/18−8	124	**581**	0.14−0.28	0.40	**546**
P18−8/18−8a	131	**578**, 610	0.21−0.31	0.33	**555**

[a]Excitation wavelength at λ_{absmax}

DOI: 10.1021/acs.macromol.5b02267
Macromolecules 2016, 49, 455−464

polymers were measured in powder form on a FT-Raman Bruker MultiRam spectrometer with a liquid nitrogen cooled Ge detector and a Nd:YAG laser at 1064 nm. Size exclusion chromatography (SEC) measurements were performed using a Pump Deltachrom (Watrex Comp.) with a Midas autosampler and two columns of MIXED-B LS PL gel, particle size 10 μm. An evaporative light scattering detector (PL-ELS-1000 from Polymer Laboratories) was used; THF was the mobile phase. Polystyrene standards were used for calibration. Mass spectra (MALDI-TOF MS) were acquired with an UltrafleXtreme (Bruker Daltonics, Bremen, Germany) in the positive ion reflectron mode. The spectra were the sum of 1000 shots with a DPSS, Nd: YAG laser (355 nm, 1000 Hz). Delayed extraction and external calibration was used.

1.1. Sample Preparation. Thin films were prepared by spin-coating from 1,2-dichlorbenzene solutions. Thin films were spin-coated onto fused silica substrates for optical studies or coated on a Pt wire electrode by dipping for electrochemical measurements. For polymer light-emitting devices (LED), polymer layers were prepared on indium−tin oxide (ITO) substrates covered with a thin layer of poly[3,4-(ethylenedioxy)thiophene]/poly(styrenesulfonate) (PEDOT:PSS). All polymer films were dried in a vacuum (10^{-3} Pa) at 373 K for 2 h. The ITO glass substrates were purchased from Merck (Germany) and PEDOT:PSS (CLEVIOS P VP AI 4083) from Heraeus Clevios GmbH (Germany). The 50 nm thick PEDOT:PSS layers were prepared by spin-coating and dried in air at 396 K for 15 min. The calcium (20 nm) and, subsequently, 60−80 nm thick aluminum electrodes were vacuum-evaporated on top of the polymer films to form LEDs. Typical active areas of the LEDs were 4−8 mm^2, precise values used for EL efficiency evaluation were determined by optical microscopy. Layer thicknesses were measured using a KLA-Tencor P-10 profilometer.

1.2. Cyclovoltammetric Measurements. Cyclic voltammetry (CV) was performed with a PA4 polarographic analyzer (Laboratory Instruments, Prague, CZ) with a three-electrode cell. Platinum (Pt) wire electrodes were used as both working and counter electrodes. A nonaqueous Ag/Ag^+ electrode (Ag in 0.1 M $AgNO_3$ solution) was used as the reference electrode. CV measurements were made in an electrolyte solution of 0.1 M tetrabutylammonium hexafluorophosphate ($TBAPF_6$) in anhydrous acetonitrile under nitrogen atmosphere. Typical scan rates were 20, 50, and 100 mV s^{-1}.

1.3. Photophysical Measurements. UV−vis spectra were measured on a PerkinElmer Lambda 35 UV/vis spectrometer. Solvents of spectroscopic grade were used. The absorption spectra of thin films were measured in the glovebox using fiber optics connected to the spectrophotometer. Steady-state PL spectra were recorded using a PerkinElmer LS55 Fluorescence spectrophotometer. The PL quantum yield of the polymer in solution was calculated relative to the quinine sulfate in 0.1 M H_2SO_4, which was used as a standard (PL quantum yield 0.577).[46]

1.4. Electroluminescence Measurements. EL spectra were recorded using an Acton Research Spectrograph with single photon-counting detection (SPEX, RCA C31034 photomultiplier). LEDs were supplied from a Keithley 237 source measure unit, which served to simultaneously record the current flowing through the sample. Current−voltage and luminance−voltage characteristics were recorded simultaneously using the Keithley 237 source measure unit and a Minolta LS110 Luminance Meter or a silicon photodiode with integrated amplifier (EG&G HUV-4000B) for the detection of total light output. A voltage signal from the photodiode was recorded with a Hewlett-Packard 34401A multimeter. All thin film preparations and the device fabrication were carried out in a glovebox under a nitrogen atmosphere.

2. Polymer Synthesis. The synthesis of the monomers, the bisphosphonate **3ab** and the dialdehyde **7ab**, and the polymers was performed in analogy to literature[1,6] and is well described in Supporting Information. All polymers were prepared under similar conditions (monomer concentration, stirring rate, reaction temperature and time). The synthesis of **P18−8/18−8** was repeated, extending the reaction time by 25 min, in order to obtain a batch (**P18−8/18−8a**) with high molecular mass, the synthesis of which is described below as an example. The details of other polymer syntheses are described in Supporting Information.

*2.1. Poly[1,4-phenyleneethynylene-1,4-(2-octadecyloxy-5-octyloxy)phenylene)-1,4-phenylethene-1,2-diyl-1,4-(2-octadecyloxy-5-octyloxy)phenylene)ethane-1,2-diyl] (**P18−8/18−8a**).* The dialdehyde **7ab** (450 mg, 0.62 mmol) and the bisphosphonate **3ab** (477 mg, 0.62 mmol) were dissolved in dry toluene (25 mL) while stirring vigorously under argon and heating under reflux (110 °C) and reacted upon the addition of an excess of potassium *tert*-butoxide (425 mg, 3.78 mmol) for 1 h and 25 min. Benzaldehyde (5 mL) and, 10 min later, toluene (30 mL) and aqueous HCl (10 wt %, 10 mL) were added to quench the reaction. The organic phase was separated and extracted several times with distilled water until the water phase became neutral (pH = 6−7). The organic layer was dried in a Dean−Stark apparatus. After filtration the toluene solution was concentrated under vacuum and precipitated in methanol. The polymer was extracted for 24 h with methanol (Soxhlett), dissolved once more in toluene, and precipitated again in methanol. Filtration and drying yielded a bright yellow fibrous polymer (630 mg, 86%).

SEC (THF): M_w = 431 000 g/mol, PDI = 4.1.

^{1}H NMR (300 MHz, $CDCl_3$, 298 K), δ/ppm: 0.87 (broad s, 12H, 4 × CH_3), 1.23−1.89 (m, 88H, 44 × CH_2), 4.07 (broad s, 8H, 4 × O−CH_2), 7.03−7.54 (m, 16H, 12 × aromatic H and 4 × vinylene H).

^{13}C NMR (75 MHz, $CDCl_3$, 298 K), δ/ppm: 14.1 ($\mathbf{C}H_3$), 22.73, 26.13, 26.32, 29.36, 29.41, 29.45, 29.50, 29.71, 29.76, 31.87, 31.97 (all $\mathbf{C}H_2$), 69.56 (O−$\mathbf{C}H_2$), 86.97 (**C≡C**), 95.35 (**C≡C**), 110.63, 114.04, 116.88, 124.38 (all H−$\mathbf{C}_{aryl}$), 126.41 (**C═C**), 126.91 (**C═C**), 128.40 ($\mathbf{C}_{aryl}$−C≡C), 131.91 ($\mathbf{C}_{aryl}$−C═C), 136.79 ($\mathbf{C}_{aryl}$−C═C), 147.17 ($\mathbf{C}_{aryl}$−O), 153.66 ($\mathbf{C}_{aryl}$−O).

IR: 3070−300 cm^{-1} (vw, H−C_{aryl} and vinylene C−H), 2950−2800 cm^{-1} (vs, C−H), 2205 cm^{-1} (w, ethynylene −C≡C−), 1689 and 1599 cm^{-1} (w, vinylene −C═C−), 1530−1360 cm^{-1} (w, aromatic C═C), 1213 and 1043 cm^{-1} (s, m, C_{aryl}−OR), 965 cm^{-1} (m, trans−C═C−).

Raman: 2950−2830 cm^{-1} (vw, −C−H), 2205 cm^{-1} (s, −C≡C−), 1626 cm^{-1} (m, vinylene −C═C−), 1600−1530 cm^{-1} (vs, aromatic −C═C−), 1240 and 1091 cm^{-1} (w, C_{aryl}−OR), 1178 cm^{-1} (s, − C−C).

UV−vis ($CHCl_3$): λ_{max}/nm = 442.

Anal. Calcd for $(C_{84}H_{124}O_4)_n$ $(1197.91)_n$ (%): C, 84.22; H, 10.43. Found: C, 84.29; H, 10.60.

DOI: 10.1021/acs.macromol.5b02267
Macromolecules 2016, 49, 455−464

■ ASSOCIATED CONTENT

Supporting Information

The Supporting Information is available free of charge on the ACS Publications website at DOI: 10.1021/acs.macromol.5b02267.

Synthesis of the monomers and polymers and characterization data (PDF)

■ AUTHOR INFORMATION

Corresponding Authors

*E-mail (V.C.): cimrova@imc.cas.cz or cimrova@gmail.com.
*E-mail (D.A.M.E.): daniel_ayuk_mbi.egbe@jku.at.

Notes

The authors declare no competing financial interest.

■ ACKNOWLEDGMENTS

We thank Czech Science Foundation for supporting this work by grants 13-26542S and P106/12/0827. D. A. M. Egbe and N. Bouguerra acknowledge the financial support of FWF through project No: I 1703-N20 and thank Prof. Sariciftci for the support during the work at the Linz Institute for Organic Solar Cells (LIOS). N.B. is grateful for financial support from the University of Bejaia, Algeria and from the African Network for Solar Energy (ANSOLE e.V.).

■ REFERENCES

(1) Egbe, D. A. M.; Ulbricht, C.; Orgis, T.; Carbonnier, B.; Kietzke, T.; Peip, M.; Metzner, M.; Gericke, M.; Birckner, E.; Pakula, T.; Neher, D.; Grummt, U.-W. *Chem. Mater.* **2005**, *17*, 6022−6032.
(2) Egbe, D. A. M.; Birckner, E.; Klemm, E. *J. Polym. Sci., Part A: Polym. Chem.* **2002**, *40*, 2670−2679.
(3) Yang, S.; Olishevski, P.; Kertesz, M. *Synth. Met.* **2004**, *141*, 171−177.
(4) Singh, R.; Singh, R. J.; Kumar, J.; Kant, R.; Kumar, V. *J. Polym. Sci., Part B: Polym. Phys.* **2010**, *48*, 1047−1053.
(5) Noël, V.; Randriamahazaka, H.; Chevrot, C. *J. Electroanal. Chem.* **2003**, *542*, 33−38.
(6) Egbe, D. A. M.; Tillmann, H.; Birckner, E.; Klemm, E. *Macromol. Chem. Phys.* **2001**, *202*, 2712−2726.
(7) Egbe, D. A. M.; Roll, C. P.; Klemm, E. *Des. Monomers Polym.* **2002**, *5*, 245−275.
(8) Tinti, F.; Sabir, F. K.; Gazzano, M.; Righi, S.; Ulbricht, C.; Usluer, O.; Pokorna, V.; Cimrova, V.; Yohannes, T.; Egbe, D. A. M.; Camaioni, N. *RSC Adv.* **2013**, *3*, 6972−6980.
(9) Mühlbacher, D.; Neugebauer, H.; Cravino, A.; Sariciftci, N. S.; van Duren, J. K. J.; Dhanabalan, A.; van Hal, P. A.; Janssen, R. A. J.; Hummelen, J. C. *Mol. Cryst. Liq. Cryst.* **2002**, *385*, 85−92.
(10) Hanif, M.; Lu, P.; Li, M.; Zheng, Y.; Xie, Z.; Ma, Y.; Li, D.; Li, J. *Polym. Int.* **2007**, *56*, 1507−1513.
(11) Heeger, A. J. *Rev. Mod. Phys.* **2001**, *73*, 681−700.
(12) Chirvase, D.; Chiguvare, Z.; Knipper, M.; Parisi, J.; Dyakonov, V.; Hummelen, J. C. *Synth. Met.* **2003**, *138*, 299−304.
(13) Nie, G.; Qu, L.; Zhang, Y.; Xu, J.; Zhang, S. *J. Appl. Polym. Sci.* **2008**, *109*, 373−381.
(14) Egbe, D. A. M.; Klemm, E. *Macromol. Chem. Phys.* **1998**, *199*, 2683−2688.
(15) Egbe, D. A. M.; Carbonnier, B.; Paul, E. L.; Mühlbacher, D.; Kietzke, T.; Birckner, E.; Neher, D.; Grummt, U.-W.; Pakula, T. *Macromolecules* **2005**, *38*, 6269−6275.
(16) Sahin, E.; Camurlu, P.; Toppare, L.; Mercore, V. M.; Cianga, I.; Yağcı, Y. *J. Electroanal. Chem.* **2005**, *579*, 189−197.
(17) Gunes, S.; Wild, A.; Cevik, E.; Pivrikas, A.; Schubert, U. S.; Egbe, D. A. M. *Sol. Energy Mater. Sol. Cells* **2010**, *94*, 484−491.
(18) Finlayson, C. E.; Ginger, D. S.; Marx, E.; Greenham, N. C. *Philos. Trans. R. Soc., A* **2003**, *361*, 363−377.
(19) Han, D.-H.; Lee, H. J.; Park, S.-M. *Electrochim. Acta* **2005**, *50*, 3085−3092.
(20) Petr, A.; Zhang, F.; Peisert, H.; Knupfer, M.; Dunsch, L. *Chem. Phys. Lett.* **2004**, *385*, 140−143.
(21) Hoven, C. V.; Yang, R.; Garcia, A.; Crockett, V.; Heeger, A. J.; Bazan, G. C.; Nguyen, T.-Q. *Proc. Natl. Acad. Sci. U. S. A.* **2008**, *105*, 12730−12735.
(22) Vorotyntsev, M. A.; Heinze, J. *Electrochim. Acta* **2001**, *46*, 3309−3324.
(23) Lee, J.-Y.; Park, S.-M. *J. Electrochem. Soc.* **2000**, *147*, 4189−4195.
(24) Gruber, J.; Li, R. W. C.; Aguiar, L. H. J. M. C.; Garcia, T. L.; de Oliveira, H. P. M.; Atvars, T. D. Z.; Nogueira, A. F. *Synth. Met.* **2006**, *156*, 104−109.
(25) Zhao, X.; Zhan, X. *Chem. Soc. Rev.* **2011**, *40*, 3728−3743.
(26) Cardona, C. M.; Li, W.; Kaifer, A. E.; Stockdale, D.; Bazan, G. C. *Adv. Mater.* **2011**, *23*, 2367−2371.
(27) Johansson, T.; Mammo, W.; Svensson, M.; Andersson, M. R.; Inganas, O. *J. Mater. Chem.* **2003**, *13*, 1316−1323.
(28) Heeger, A. J. *Chem. Soc. Rev.* **2010**, *39*, 2354−2371.
(29) Egbe, D. A. M.; Bader, C.; Klemm, E.; Ding, L.; Karasz, F. E.; Grummt, U.-W.; Birckner, E. *Macromolecules* **2003**, *36*, 9303−9312.
(30) Tore, N.; Parlak, E. A.; Usluer, O.; Egbe, D. A. M.; San, S. E.; Aydogan, P. *Sol. Energy Mater. Sol. Cells* **2012**, *104*, 39−44.
(31) Tekin, E.; Egbe, D. A. M.; Kranenburg, J. M.; Ulbricht, C.; Rathgeber, S.; Birckner, E.; Rehmann, N.; Meerholz, K.; Schubert, U. S. *Chem. Mater.* **2008**, *20*, 2727−2735.
(32) Carbonnier, B.; Egbe, D. A. M.; Birckner, E.; Grummt, U.-W.; Pakula, T. *Macromolecules* **2005**, *38*, 7546−7554.
(33) Egbe, D. A. M.; Tekin, E.; Birckner, E.; Pivrikas, A.; Sariciftci, N. S.; Schubert, U. S. *Macromolecules* **2007**, *40*, 7786−7794.
(34) Liu, Y.; Liu, M. S.; Jen, A. K.-Y. *Acta Polym.* **1999**, *50*, 105−108.
(35) Tekin, E.; Wijlaars, H.; Holder, E.; Egbe, D. A. M.; Schubert, U. S. *J. Mater. Chem.* **2006**, *16*, 4294−4298.
(36) Egbe, D. A. M.; Roll, C. P.; Birckner, E.; Grummt, U.-W.; Stockmann, R.; Klemm, R. *Macromolecules* **2002**, *35*, 3825−3837.
(37) Carbonnier, B.; Pakula, T.; Egbe, D. A. M. *J. Mater. Chem.* **2005**, *15*, 880−890.
(38) (a) Weder, C.; Wrighton, M. S. *Macromolecules* **1996**, *29*, 5157−5165. (b) Wang, F.; He, F.; Xie, Z. O.; Li, Y. P.; Hanif, M.; Li, M.; Ma, Y. *Macromol. Chem. Phys.* **2008**, *209*, 1381−1388.
(39) Cimrová, V.; Neher, D.; Kostromine, S.; Bieringer, Th. *Macromolecules* **1999**, *32*, 8496−8503.
(40) Blatchford, J. W.; Jessen, S. W.; Lin, L.-B.; Gustafson, T. L.; Fu, D.-K.; Wang, H.-L.; Swager, T. M.; MacDiarmid, A. G.; Epstein, A. J. *Phys. Rev. B: Condens. Matter Mater. Phys.* **1996**, *54*, 9180−9189.
(41) Ding, L.; Egbe, D. A. M.; Karasz, F. E. *Macromolecules* **2004**, *37*, 6124−6131.
(42) Cimrová, V.; Neher, D.; Remmers, M.; Kmínek, I. *Adv. Mater.* **1998**, *10*, 676−680.
(43) (a) Cimrová, V.; Výprachtický, D. *Appl. Phys. Lett.* **2003**, *82*, 642−644. (b) Cimrová, V.; Výprachtický, D. *Macromol. Symp.* **2004**, *212*, 281−286.
(44) Mikroyannidis, J. A.; Barberis, V. P.; Výprachtický, D.; Cimrová, V. *J. Polym. Sci., Part A: Polym. Chem.* **2007**, *45*, 809−821.
(45) Cimrová, V.; Výprachtický, D.; Hoerhold, H.-H. *J. Polym. Sci., Part A: Polym. Chem.* **2011**, *49*, 2233−2244.
(46) Eastman, J. W. *Photochem. Photobiol.* **1967**, *6*, 55−72.

DOI: 10.1021/acs.macromol.5b02267
Macromolecules 2016, 49, 455−464